Hong Shen
School of Mechanical Engineering,
Shanghai Jiao Tong University,
Shanghai 200240, China;
State Key Laboratory of Mechanical System and Vibration,
Shanghai 200240, China
e-mail: sh_0320@sjtu.edu.cn

Yutao Zheng
School of Mechanical Engineering,
Shanghai Jiao Tong University,
Shanghai 200240, China

Han Wang
School of Mechanical Engineering,
Shanghai Jiao Tong University,
Shanghai 200240, China

Zhenqiang Yao
School of Mechanical Engineering,
Shanghai Jiao Tong University,
Shanghai 200240, China;
State Key Laboratory of Mechanical System and Vibration,
Shanghai 200240, China

Heating Position Planning in Laser Forming of Single Curved Shapes Based on Probability Convergence

Inverse problem in laser forming involves the heating position planning and the determination of heating parameters. In this study, the heating positions are optimized in laser forming of single curved shapes based on the processing efficiency. The algorithm uses a probability function to initialize the heating position that is considered to be the bending points. The optimization process is to minimize the total processing time through adjusting the heating positions by considering the boundary conditions of the offset distances, the minimum bending angle, and the minimum distance between two adjacent heating positions. The optimized results are compared with those obtained by the distance-based model as well as the experimental data. [DOI: 10.1115/1.4032394]

Keywords: probability convergence, heating position planning, laser forming, single curved shape

1 Introduction

Laser forming is a new technique that uses laser beam as a heat source to deform plates made of different materials, such as steels, titanium alloys, and ceramics. During the process of laser forming, the thermal stress induced by the nonuniform temperature distribution is beyond the yield stress of the material, which can produce plastic deformations. Laser forming has many advantages over the traditional forming technologies. It requires no tools or external forces in the process. With the flexibility of laser beam delivering and the use of numerical control systems, it is easier to incorporate laser forming into various manufacturing systems. Material degradation in laser forming is typically limited to a very tiny layer of the irradiated surface due to highly concentrated beam power and short interaction time [1].

Laser forming attracts much attention and a lot of work has been accomplished. Geiger and Vollertsen [2] identified three key mechanisms to explain the thermomechanical behaviors in laser forming, namely, temperature gradient mechanism (TGM), buckling mechanism (BM), and upsetting mechanism. Some analytical models have been developed for determining the bending angle induced by the straight-line scan in laser forming. For instance, Kyrsanidi et al. [3] presented a parametric mathematical model that considers plastic bending during heating. A similar model was proposed by Cheng and Lin [4]. Shen et al. [5] derived a formula of bending angle in laser forming based on the assumptions that the plastic deformation is generated only during heating, and during cooling only the elastic deformation occurs. Numerical simulations have also been performed using various commercial codes for evaluating the performance of laser forming. Hu et al. [6] performed a three-dimensional (3D) finite element method (FEM) simulation that included a nonlinear, transient, indirect coupled, thermal-structural analysis accounting for the geometric and material nonlinear properties. Guan et al. [7] performed a numerical investigation on the laser forming of prebent plates using the thermal elastoplastic FEM. Liu et al. [8] used FEM to investigate the effects of various prestresses on mechanical behavior in laser forming dominated by BM.

Most of the work mentioned above was focused on a single bending angle of laser forming. Very few works were related to the inverse problem of laser forming. The task of free curve laser forming is to determine a set of process parameters, such as laser scanning paths, laser power, and scanning speed. A distance-based method and an angle-based method were used for generating the laser scanning paths and the bending angles of each path [9]. These two methods have been applied to 3D laser forming [10] and flame forming considering the arc shape in the flame heating areas [11]. Abed et al. [12] put forward the scan strategies based on contours of constant height of a surface using TGM. Yu et al. [13] presented an algorithm for flatting a smooth continuous curved surface into a planar shape. The process is modeled by creating in-plane strains from the curved surface to its planar development based on differential geometry. Liu et al. [14] then used this algorithm for planning of scan paths according to the distribution of in-plane strains. Cheng and Yao [15] presented the strain field by using large-deformation, elastic finite element analysis methods. The scan path is generated using minimal principal strains of in-plane directions based on the strain field. However, their approach to heating path determination is not optimized based on the processing time.

The objective of this paper is to develop an optimization method that can minimize the processing time in laser forming of single curved shapes. A probability-based method is proposed to generate and optimize the heating positions. Moreover, the results obtained by the present model are compared with those by the distance-based model [9] as well as the experimental data.

2 Description of the Problem

Figure 1 shows how a flat plate is bent into a single curved shape by the laser forming process. In this study, the edge effects (the variation of bending angle along the heating line) are ignored [9]. Therefore, a 3D laser forming can be simply treated as a two-

Manuscript received November 2, 2015; final manuscript received December 16, 2015; published online June 20, 2016. Assoc. Editor: Matteo Strano.

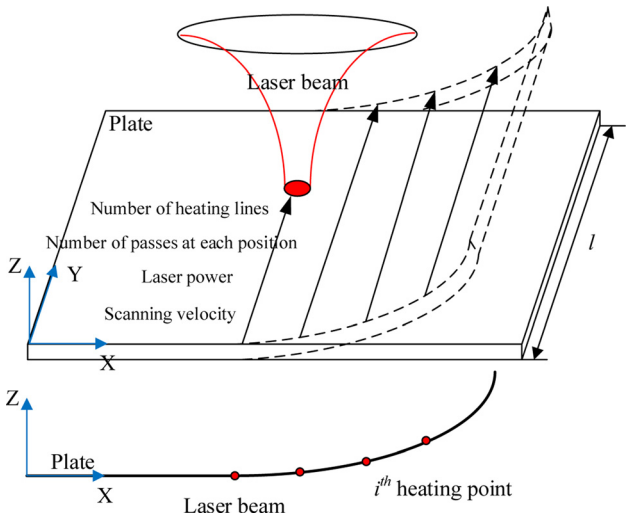

Fig. 1 Schematic of laser forming process of a single curve shape

dimensional forming problem. In other words, the heating lines along the y-direction can be treated as the heating points in x–z plane.

To get a curved shape from the flat sheet metal, two questions need to be answered. One is where to heat and the other is how much energy to apply to the heating point/line, that is, the heating location and the bending angle at each heating position. Note that the magnitude of the bending angle is determined by the laser power, scanning velocity, and number of passes at each heating position. Therefore, the processing time for laser forming of the curved shape can be expressed as

$$t_t = \sum_{i=1}^{k} t_i n_i \tag{1}$$

where t_t is the total heating time for the process, k is the number of the heating points/lines, and n_i is the number of passes at the ith heating position, $t_i = l/v_i$ is the heating time for one scan at the ith heating position, l is the width of the plate, and v_i is the scanning velocity at the ith heating position.

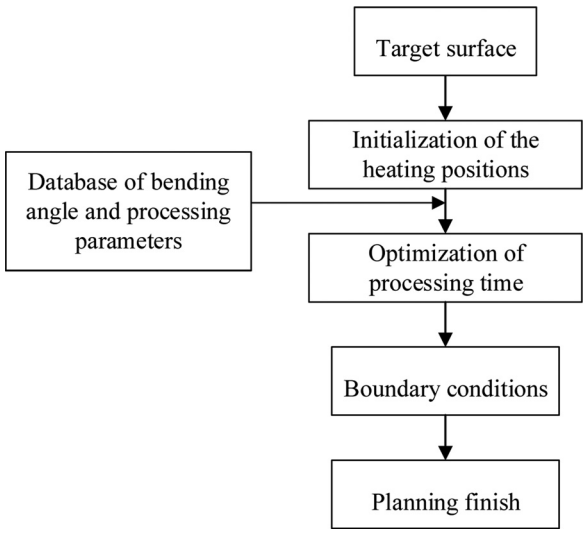

Fig. 2 Overall strategy for planning heating positions based on the processing time

In order to reduce the processing time, the following three ways can be used:

(1) decrease the number of the heating positions (k)
(2) decrease the heating time (t_i) (i.e., improve the scanning velocity (v_i)) at the i^{th} heating position
(3) decrease the number of passes (n_i) at the i^{th} heating position

Figure 2 summarizes the algorithms for planning the heating positions in laser forming of single curved shapes based on the processing efficiency.

3 Heating Position Planning

3.1 Initialization of the Heating Positions. It is known that the radius of curvature is one of the important geometrical parameters for a curve. According to the deformation behavior of laser forming, the heating point generally exists where the radius of curvature is relative small, which means that the probability of the appearance of the heating point is larger. In this study, a weight function with the radius of curvature is induced to represent the probability of being the heating point on the target curve. In order to facilitate the calculation, the weight function needs to meet some of the requirements that are as follows:

(1) Each point on the target curve has only one specific weight value of this function.
(2) When the weight value of one point on the target curve is higher than that of another point, this point has a larger probability of being the heating point.
(3) The difference between the maximum and minimum of this function is not too large to avoid the convergent problem in the calculation.

Therefore, the weight function is defined as

$$f(x) = \frac{1}{\ln(r(x))} \tag{2}$$

where x is the x-direction coordinate of the point on the curve, and $r(x)$ is the radius of curvature at this point. Hence, the probability p of the heating point existing in an interval $[x_1, x_2]$ on the target curve is expressed as

$$p = \frac{\int_{x_1}^{x_2} f(x)dx}{\int_{x_0}^{x_n} f(x)dx} \tag{3}$$

where x_0 is the x-direction coordinate of the start point on the target curve, such as $x_0 = 0$, x_n is the x-coordinate of the end point on the target curve, and x_1 and x_2 are the x-direction coordinates of the left and right points for an interval on the target curve, respectively.

Considering the continuity of the weight function, the target curve can be divided into n sections (Fig. 3) and each section has the same integral quantity, such as

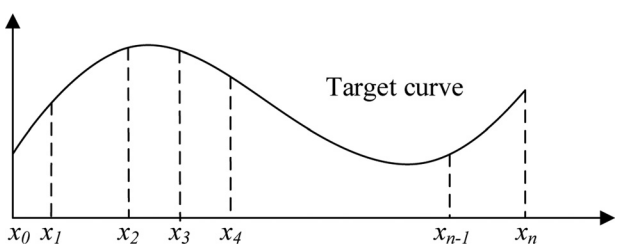

Fig. 3 The partition of the target curve

$$\frac{\int_{x_0}^{x_1} f(x)dx}{\int_{x_0}^{x_n} f(x)dx} = \frac{\int_{x_1}^{x_2} f(x)dx}{\int_{x_0}^{x_n} f(x)dx} = \cdots = \frac{\int_{x_{n-1}}^{x_n} f(x)dx}{\int_{x_0}^{x_n} f(x)dx} \tag{4}$$

According to the definition of the probability p, the target curve is divided into n sections and each section has the heating point with the same probability, which implies that the distribution of the heating points is initialized.

3.2 Boundary Conditions. After initializing the distribution of the heating points along the target curve, the heating points satisfy the boundary conditions as follows.

3.2.1 Error Band ($\pm d$). The error band is employed in the forming process, which is similar to the tolerance zone in machining process. The designed curve is generated by the heating positions at which the bending angle exists and it should locate between the upper and lower boundaries of the target curve. If the designed curve is beyond the offset distance (Fig. 4), the new heating position is added between the two existing heating positions. In this study, a simple way is adopted, in which the new point C is located at the middle of points A and B in x-direction.

3.2.2 Minimum Bending Angle (α_{min}). The relationship between the bending angle and the laser processing parameters including laser power and scanning velocity is the basis for planning the laser heating position. When a bending angle at some heating position is smaller than the minimum bending angle in the database, this heating position will be removed, which means that the two heating positions near the removed heating position are reconnected, as shown in Fig. 5.

3.2.3 Minimum Distance Between Two Heating Positions (l_0). In general, the smaller the distance between two heating points, more precise the desired shapes can be formed and lower energy input is required for each path. On the other hand, it will take longer to form the shapes and the adjacent heating points can no longer be assumed to be independent with each other. The independence is paid attention to because the heating position planning is based on a database which is constructed using independent scans.

If the distance between two heating points A and B is smaller than the minimum distance l_0, the heating point A can move to A′ (Fig. 6(*a*)), or the heating point B can move to B′ (Fig. 6(*b*)), or the two heating points move to the left and right, respectively, along the target curve (Fig. 6(*c*)), depending on the distribution of the heating points.

3.3 Optimization Based on the Probability Convergence. After initializing the distribution of the heating points and defining the boundary conditions, the heating location can be optimized by adjusting the heating points according to the total processing time.

For some heating point $A(x_i, z)$ on the target curve with a section $(x_i - a/2, x_i + a/2)$ and a random number δ in the section

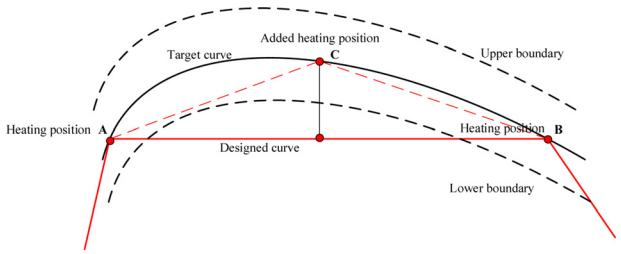

Fig. 4 Boundary condition: error band

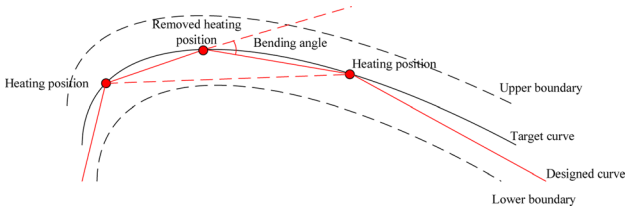

Fig. 5 Boundary condition: minimum bending angle

of (0, 1], the integral equation (5) is used to create the new heating position based on Eq. (3)

$$\int_{x_i - a/2}^{x_i'} f(x)dx = \delta \int_{x_i - a/2}^{x_i + a/2} f(x)dx \tag{5}$$

where a is a distance (normally, it can be taken as one-third of interval length), and x_i' is the x-direction coordinate of the modified heating point in the section of $(x_i - a/2, x_i + a/2)$ on the target curve. Based on Eq. (5), each initialized heating point is modified step-by-step, and the boundary conditions are also checked at each step. Then, the total processing time is compared between the initialized heating positions and the modified heating positions to revalue the weight, as shown in Fig. 7. When the boundary conditions are not satisfied or processing time for the new heating position is larger than the last heating position, the weight function is redefined as $f(x) = A(1/\ln(r(x)))$ with $0 < A < 1$. If the new heating position has more efficiency, the coefficient A in $f(x)$ is larger than 1.

The optimization of the heating points out of the target curve means that the heating points do not move along the target curve

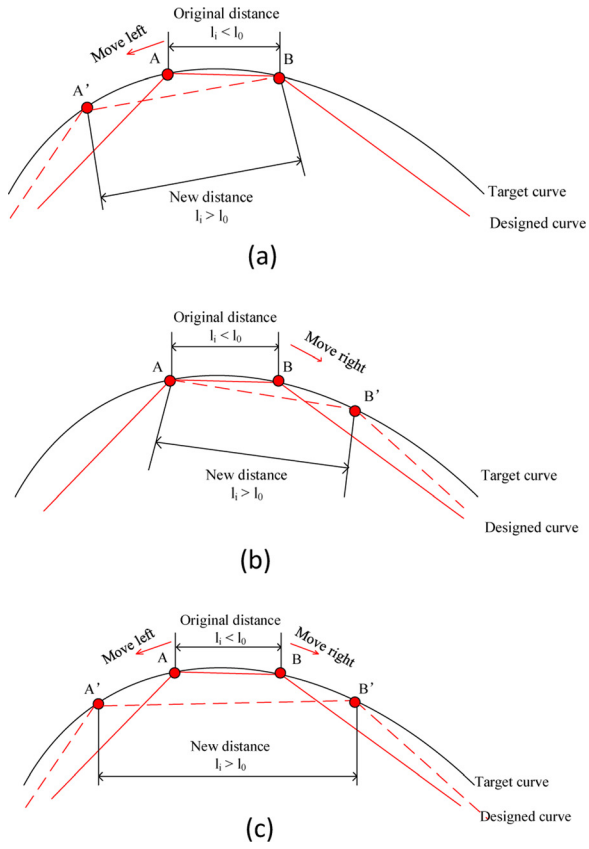

Fig. 6 Boundary condition: minimum distance between two heating positions. (*a*) Move left, (*b*) move right, and (*c*) move both sides.

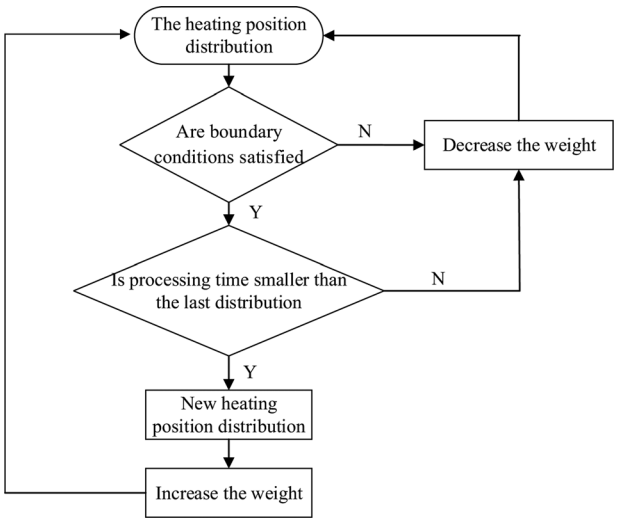

Fig. 7 Flowchart of generating the new heating position

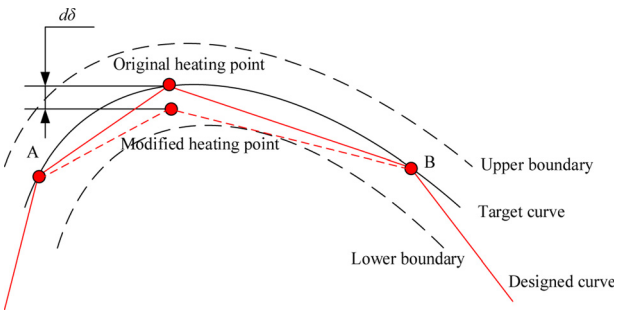

Fig. 8 Heating point moving between the error band

but in the space between the error bands of the curve. This part of optimization is pretty similar to the optimization of the heating points along the target curve. For each modification, a distance $d\delta$ in z direction between the original heating point and the modified heating point is defined by a random number δ in the section of $[-1, 1]$ with the maximum offset distance d, as shown in Fig. 8.

4 Case Study and Experimental Validation

4.1 Database of Bending Angle. After the heating points and bending angles are achieved, the processing parameters are selected to bend the plate to a given angle at each heating point. In this study, three control parameters including laser power, scanning velocity, and number of passes are related to the bending angle.

A fiber laser with the maximum laser power of 280 W with a wavelength of 1070 nm was used, and the selected samples were 304 stainless steel coupons with dimension of $100 \times 100 \times 2$ mm^3, as shown in Fig. 9(*a*). The selection of the processing parameters is under the condition that the maximum temperature is below the melting temperature of the material, and the minimum bending angle can be measured. The laser beam profile is Gaussian distribution and the beam diameter is kept constant about 2 mm. The parameters used are 210, 225, 245, 260, and 280 W for the laser power, 24, 28, 32, 36, 38, and 40 mm/s for the scanning velocity. Each combination of the processing parameters was performed for three samples. In order to better measure the deformed angle, the laser displacement sensor was used to scan on the nonirradiated surface (Fig. 9(*b*)). The average bending angle is adopted through three locations scanned by the sensor to reduce the error caused by the edge effects in the laser forming, as shown in Fig. 9(*c*). Figure 10(*a*) shows the relationship of laser power, scanning velocity, and bending angle via experimental data of single straight-line heating using the response surface method. The relationship can be approximately expressed as

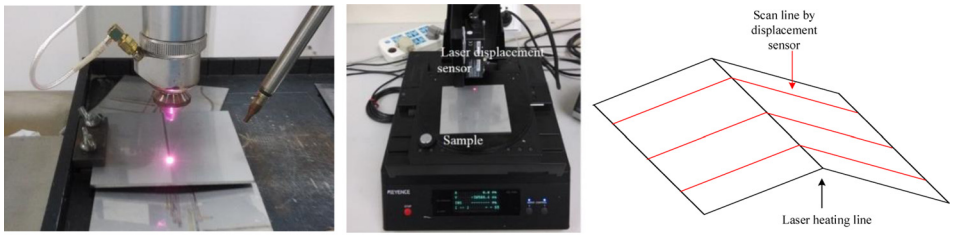

Fig. 9 Experimental setup of laser forming: (*a*) laser heating, (*b*) displacement sensor, and (*c*) measurement scheme

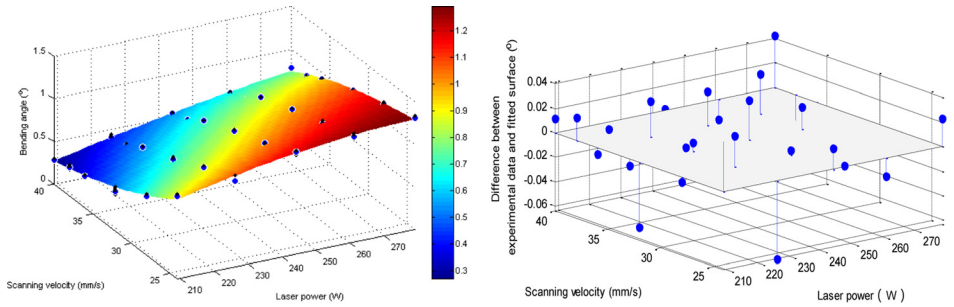

Fig. 10 Experiment-determined relationship between laser power, scanning velocity, and bending angle: (*a*) fitted surface by RSM (R^2: 0.9873) and (*b*) error distribution (RMSE: 0.03259 deg)

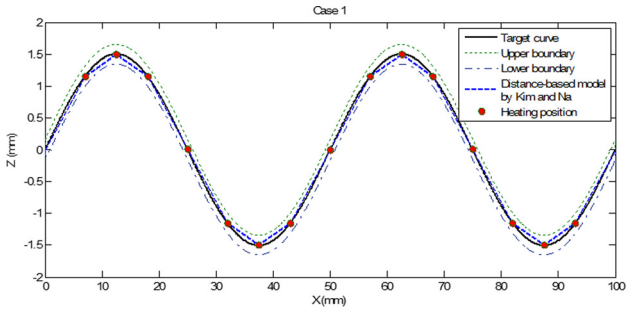

Fig. 11 Case 1: Heating position planning based on the distance-based model

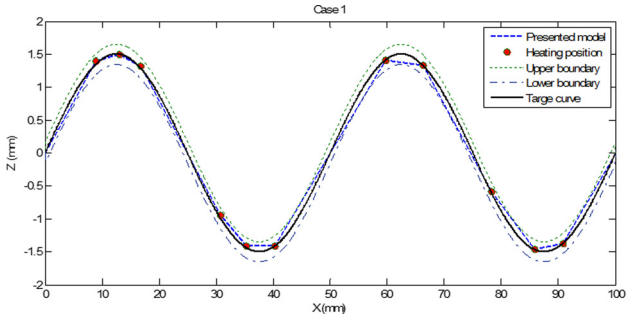

Fig. 12 Case 1: Heating position planning based on the present model

$$\alpha(P,V) = 6.793 - 0.01468P - 0.5565V + 0.0014PV + 0.0104V^2 \quad (6)$$

The deviation between the experimental data and the fitted surface is shown in Fig. 10(*b*), from which a good agreement between them can be observed.

4.2 Case Study Examples. *Case 1*: The target curve is a sine curve, $z = 1.5\sin(4\pi x/100)$ mm with the boundary conditions that the offset distance d in error band is 0.1 mm, the minimum bending angle is 0.003 rad, and the minimum distance l_0 between the two heating points is 3 mm, which is three times of laser beam radius.

The distance-based method [9] uses the maximum distance between the given sheet metal and the target shape as a criterion for a new heating point. The procedure of the distance-based criterion algorithm is as follows. A point on the target surface that has the maximum distance between the target surface and the formed line is found. If the maximum distance is larger than the set offset distance, the maximum distance point is adopted as a new forming position.

Based on the distance-based model, 15 heating positions are planned along the target curve as shown in Fig. 11. The laser power, scanning velocity, and number of passes at each heating position are listed in Table 1. Due to the geometrical shape of the curve, the heating positions are located on both sides represented by −1 and 1. Therefore, the total processing time is evaluated only considering the time of laser heating. It is noted that the

Table 1 Case 1: Processing time by the distance-based model

Heating position no., k	Scanning velocity (mm/s)	Laser power (W)	Top/bottom surface	Number of passes, n	Heating location, x (mm)	Processing time (s)
1	30	252	−1	7	7.1	11.67
2	29	252	−1	8	12.6	13.79
3	30	252	−1	7	18.1	11.67
4	0	0	−1	1	25.2	0
5	30	252	1	7	32.3	11.67
6	29	252	1	8	37.8	13.79
7	30	252	1	7	43.3	11.67
8	0	0	1	1	50.4	0
9	30	252	−1	7	57.5	11.67
10	29	252	−1	8	63.0	13.79
11	30	252	−1	7	68.5	11.67
12	0	0	−1	1	75.6	0
13	30	252	1	7	82.7	11.67
14	29	252	1	8	88.2	13.79
15	30	252	1	7	93.7	11.67
$k = 15$	$\bar{v} = 29.7$			$\sum n = 91$		$t_t = 148.52$

Table 2 Case 1: Processing time by the present model

Heating position no., k	Scanning velocity (mm/s)	Laser power (W)	Top/bottom surface	Number of passes, n	Heating location, x (mm)	Processing time (s)
1	30	252	−1	9	8.9	15.00
2	31	252	−1	5	13.0	8.06
3	31	252	−1	8	16.8	12.90
4	32	252	1	4	30.8	6.25
5	29	252	1	7	35.3	12.07
6	28	252	1	9	40.3	16.07
7	29	252	−1	10	59.7	17.24
8	30	252	−1	10	66.3	16.67
9	30	252	1	3	78.2	5.00
10	30	252	1	9	85.8	15.00
11	28	252	1	8	90.8	14.29
$k = 11$	$\bar{v} = 29.8$			$\sum n = 82$		$t_t = 138.55$

Table 3 Case 2: Processing time by the distance-based model

Heating position no., k	Scanning velocity (mm/s)	Laser power (W)	Top/bottom surface	Number of passes, n	Heating location, x (mm)	Processing time (s)
1	34	252	−1	4	5.1	5.88
2	30	252	−1	3	10.2	5.00
3	37	252	−1	2	15.3	2.70
4	33	252	1	1	25.0	1.52
5	38	238	1	2	30.1	2.63
6	38	252	1	2	35.2	2.63
7	39	224	−1	1	50.0	1.28
8	34	252	−1	1	60.2	1.47
9	37	210	1	1	75.0	1.35
$k=9$	$\bar{v}=35.6$			$\sum n=17$		$t_t=24.47$

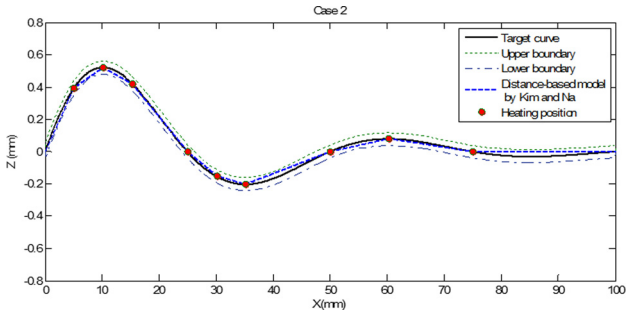

Fig. 13 Case 2: Heating position planning based on the distance-based model

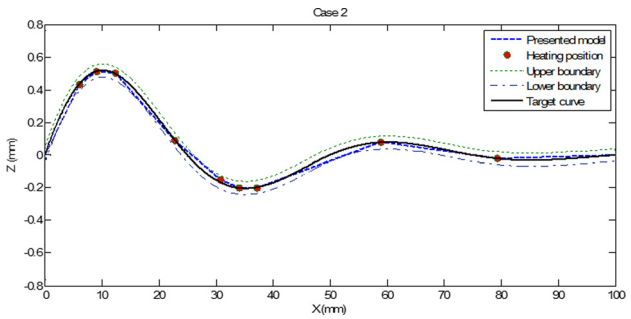

Fig. 14 Case 2: Heating position planning based on the present model

bending angles at the heating positions 4, 8, and 12 are zero, and no laser energy is applied to these heating locations, which implies that the redundant heating positions may exist using the distance-based model.

Figure 12 shows the heating position planning by the present model. It is clearly shown that the number of heating positions is 12, which is less than the number planned by the distance-based model. The heating positions are mainly located at the area of the small curvature radius of the target curve. Moreover, some heating locations, for example, heating position number 1, 3, 4, and 5, are not on the target curve, which is explained in Fig. 8. Comparing Table 1 with Table 2, the total heating time (t_t) is reduced using the present model. The main reason for this is that the total number of passes ($\sum n$) decreases due to the use of less heating positions and better heating locations although the two methods have very similar average scanning velocity. Therefore, the total processing time can be reduced to 138.55 s, and the processing efficiency is improved by 6.71%.

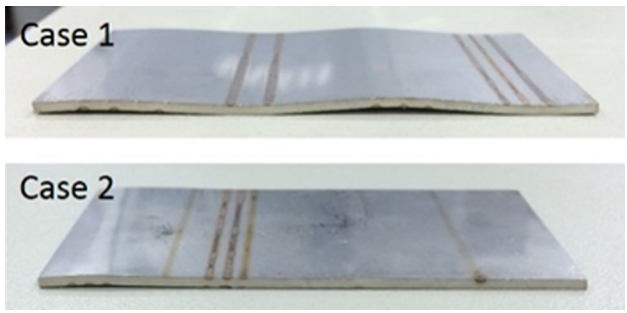

Fig. 15 Experimental samples for cases 1 and 2

Case 2: The target curve is a decayed sine curve, $z = (10/4\pi)e^{-1.2\pi x/100}\sin(4\pi x/100)$ with similar boundary conditions as used in case 1 except that the offset distance d in error band is 0.05 mm.

It can be seen from Figs. 13 and 14 that the present model and the distance-based model have the same heating position number but different distributions. Also, the average velocity in the distance-based model is larger than that in the present model. However, the processing efficiency by the present model is 5.35% higher when compared to the distance-based model due to the

Table 4 Case 2: Processing time by the present model

Heating position no., k	Scanning velocity (mm/s)	Laser power (W)	Top/bottom surface	Number of passes, n	Heating location, x (mm)	Processing time (s)
1	29	252	−1	3	6	5.17
2	29	252	−1	2	9.1	3.45
3	37	252	−1	3	12.3	4.05
4	35	224	1	1	22.8	1.43
5	29	252	1	1	30.7	1.72
6	28	252	1	1	34.0	1.79
7	37	252	1	1	37.2	1.35
8	34	224	−1	2	58.8	2.94
9	40	224	1	1	79.2	1.25
$k=9$	$\bar{v}=33.1$			$\sum n=15$		$t_t=23.16$

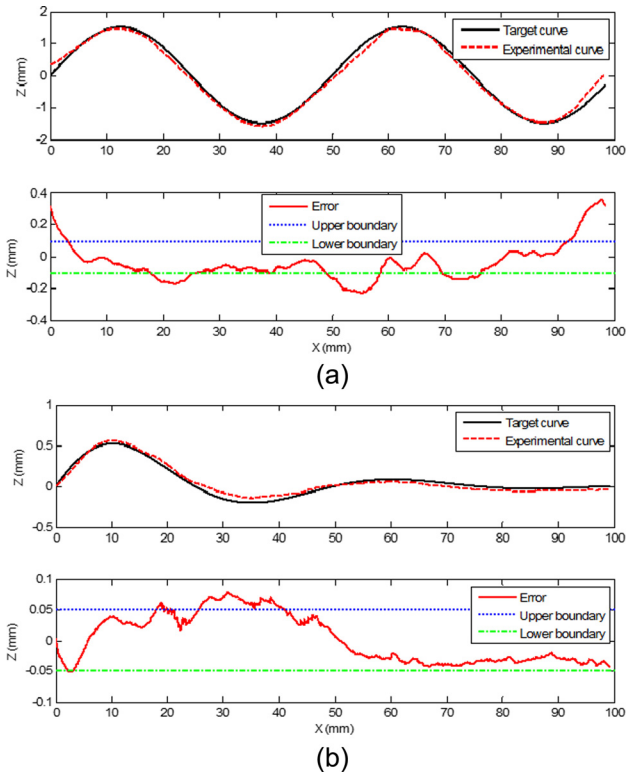

Fig. 16 Experimental results based on the present model: (*a*) case 1 and (*b*) case 2

reduced total number of scanning passes, as shown in Tables 3 and 4.

Figure 15 shows the experimental results of forming surfaces for cases 1 and 2. The measured surface profiles are compared with the target surfaces (see Fig. 16), which shows that the deformed profile is mostly between the upper and lower boundaries. However, the two ends of the sample have a relative large error for case 1 due to the edge effects in laser forming. An error between these results exists around $\pm 10\%$, which may be caused by the small deviation at single scan and the assumption that the repeated scans at the same position are independent and have the same bending angle.

5 Conclusions

The optimization in laser forming of single curved shapes is analyzed by defining a probability function. The algorithm uses a probability function to initialize the heating position being the bending points. The optimization process is to minimize the total processing time through adjusting the heating positions, considering the boundary conditions of the offset distance, the minimum bending angle, and the minimum distance between two adjacent heating positions. The optimized results are compared with the distance-based model and experimental data, which demonstrates that the present method is more efficient, and the corresponding results are in a reasonable agreement with the experimental data. However, some regions of the deformed shape are beyond the designed error band due to the variation of laser forming process. Therefore, a feedback control system is required to reduce the overall error during the forming process in future.

References

[1] Shen, H., Shi, Y. J., and Yao, Z. Q., 2006, "Numerical Simulation of the Laser Forming of Plates Using Two Simultaneous Scans," Comput. Mater. Sci., **37**(3), pp. 239–245.

[2] Geiger, M., and Vollertsen, F., 1993, "The Mechanisms of Laser Forming," CIRP Ann., **42**(1), pp. 301–304.

[3] Kyrsanidi, A. K., Kermanidis, T. B., and Pantelakis, S. G., 2000, "An Analytical Model for the Prediction of Distortions Caused by the Laser Forming Process," J. Mater. Process. Technol., **104**(1–2), pp. 94–102.

[4] Cheng, P. J., and Lin, S. C., 2001, "An Analytical Model to Estimate Angle Formed by Laser," J. Mater. Process. Technol., **108**(3), pp. 314–319.

[5] Shen, H., Yao, Z. Q., Shi, Y. J., and Hu, J., 2006, "An Analytical Formula for Estimating the Bending Angle by Laser Forming," Proc. Inst. Mech. Eng., Part C, **220**(2), pp. 243–247.

[6] Hu, Z., Kovacevic, R., and Labudovic, M., 2002, "Experimental and Numerical Modeling of Buckling Instability of Laser Sheet Forming," Int. J. Mach. Tools Manuf., **42**(13), pp. 1427–1439.

[7] Guan, Y. J., Sun, S., Zhao, G. Q., and Luan, Y. G., 2003, "Finite Element Modeling of Laser Bending of Pre-Loaded Sheet Metals," J. Mater. Process. Technol., **142**(2), pp. 400–407.

[8] Liu, J., Sun, S., and Guan, Y. J., 2009, "Numerical Investigation on the Laser Bending of Stainless Steel Foil With Pre-Stresses," J. Mater. Process. Technol., **209**(3), pp. 1580–1587.

[9] Kim, J., and Na, S. J., 2003, "Development of Irradiation Strategies for Free Curve Laser Forming," Opt. Laser Technol., **35**(8), pp. 605–611.

[10] Kim, J., and Na, S. J., 2009, "3D Laser-Forming Strategies for Sheet Metal by Geometrical Information," Opt. Laser Technol., **41**(6), pp. 843–852.

[11] Seong, W. J., Ahn, J., Na, S. J., Han, M. S., and Jeon, Y. C., 2010, "Geometrical Approach for Flame Forming of Single Curved Ship Hull Plate," J. Mater. Process. Technol., **210**(13), pp. 1811–1820.

[12] Abed, E., Edwardson, S. P., Dearden, G., and Watkins, K. G., 2005, "Closed Loop 3-Dimensional Laser Forming of Developable Surfaces," International Workshop on Thermal Forming, Bremen, Germany, Apr. 13–14, pp. 1–21.

[13] Yu, G. X., Patrikalakis, N. M., and Maekawa, T., 2000, "Optimal Development of Doubly Curved Surfaces," Comput. Aided Geom. Des., **17**(6), pp. 545–577.

[14] Liu, C., Yao, Y. L., and Srinivasan, V., 2004, "Optimal Process Planning for Laser Forming of Doubly Curved Shapes," ASME J. Manuf. Sci. Eng., **126**(1), pp. 1–9.

[15] Cheng, J., and Yao, Y. L., 2004, "Process Design of Laser Forming for Three-Dimensional Thin Plates," ASME J. Manuf. Sci. Eng., **126**(2), pp. 217–255.